Research Article Vol. 29, No. 6 / 15 March 2021 / Optics Express 9190

Optics EXPRESS

# Optically transparent microwave absorber based on water-based moth-eye structures

H. KWON,[1,2,7] G. D'AGUANNO,[1,3,4,8] AND A. ALÚ[1,5,6,9]

[1]Department of Electrical and Computer Engineering, The University of Texas at Austin, Austin, Texas 78712, USA
[2]Department of Electrical and Communication Engineering, Republic of Korea Air Force Academy, Chungbuk 28187, Republic of Korea
[3]Department of Computer Science and Electrical Engineering, University of Maryland, 1000 Hilltop Circle, Baltimore, MD 21250, USA
[4]The Johns Hopkins University, Applied Physics Laboratory, 11100 Johns Hopkins Rd., Laurel, MD 20723, USA
[5]Photonics Initiative, Advanced Science Research Center, City University of New York, New York, NY 10031, USA
[6]Graduate Center of the City University of New York, New York, NY 10016, USA
[7]hoyeong3958@utexas.edu
[8]giuseppe.daguanno@jhuapl.edu
[9]aalu@gc.cuny.edu

**Abstract:** We propose an approach to realize an optically transparent microwave absorber based on water-based moth-eye metamaterial structures. The absorber is made of a periodic array of properly shaped glass caps infiltrated with distilled water. Analytical calculations and numerical simulations show that the water-based metamaterial absorbs electromagnetic waves over a wide spectral band ranging from 4GHz to well above 120GHz, showing absorption levels close to 100% for incident radiation that ranges from normal to grazing angles, for both TE and TM polarizations. Yet, the structure is optically transparent, offering exciting opportunities in a variety of civil and military applications, such as for camouflage and shielding systems and in energy harvesting structures.



## 1. Introduction

Radar absorbing materials (RAMs) are materials designed and shaped to absorb incident radio-frequency (RF) radiation. There are currently several ways to realize RAMs [1–4], e.g., a) iron ball paint absorbers, which consists of tiny iron particles that are coated with carbonyl iron or ferrite. These particles share may similarities with ferrite grains and carbon black particles [carbonyl iron spherical particles, and/or crystalline graphite particles] embedded in the neoprene polymer sheets used in stealth aircrafts; b) foam absorbers, used for example in anechoic chambers, consisting of urethane foam also loaded with carbon black particles and cut into square pyramids to reduce scattering and maximize absorption. Nanoporous foams form another type of effective foam absorbers, fabricated with lossy materials such as alumina [5]; c) resonant absorbers, or called quarter wavelength absorbers, which include Dallenbach layers, Salisbury screens [6] and Jaumann layers. In this class of materials, the power is absorbed using wave-interfering techniques to cancel the reflected waves. All the above mentioned RAMs are generally not transparent in the visible and near-IR range. On the other hand, there are many applications, both military and civilians, such as camouflage and shielding systems or photovoltaic systems, in which optically transparent absorbers would be highly desirable. To this end, recent works have demonstrated the potential of using graphene in a Salisbury screen configuration [7–12] to realize an optically transparent microwave absorber, exploiting the fact that graphene is a good conductor at lower frequencies, and it is almost transparent at optical frequencies. However, there

#418220 https://doi.org/10.1364/OE.418220
Journal © 2021 Received 8 Jan 2021; revised 19 Feb 2021; accepted 20 Feb 2021; published 9 Mar 2021

Optics EXPRESS

are some serious drawbacks that may hamper the use of graphene for these applications. First, a single layer of graphene may arguably not be sufficient to absorb significantly large amounts of power without triggering unwanted side effects, such as nonlinearities. Multiple layers may create issues at higher frequencies, considering that each atomic layer of graphene actually absorbs around 2% of light. Another issue is the difficulty in growing high-quality graphene layers, which may in practice hinder the applicability of this concept in practical, large-scale applications. Most importantly, the approaches proposed so far using graphene rely on designs based on Salisbury screen configurations, which are well known to have a limited bandwidth in terms of the frequencies and incident angles over which good absorption can be achieved.

Subwavelength structures periodically patterned on the surface of optically transparent materials have been known to reduce Fresnel reflections since the time of Lord Rayleigh [13]. In particular, moth-eye antireflection coatings are structures made of a periodic array of pillars of various shapes (pyramidal, conical, *etc.*) on a substrate, and owe their name to the similarity with the microstructures on the eyes of nocturnal moths [14,15]. In this kind of structures, the subwavelength periodic pattern creates an effective buffer layer with an effective refractive index that reduces the impedance mismatch between the incident medium (generally air) and the substrate. In other words, the effective buffer layer created by the subwavelength pattern removes the abrupt index discontinuity that would otherwise be present at the incident medium/substrate interface. These structures are currently used in many applications, such as photovoltaics [16], LEDs [17] and fiber optics [18], just to name a few. Recently, impedance-matched metal-dielectric metamaterials in the shape of moth-eye structures have been demonstrated to yield polarization independent absorption level close to 100% from normal up to grazing incident angles in the range from 400 nm to 6μm [19].

In this paper, we propose an approach to realize optically transparent microwave absorbers that overcome the challenges of these previous schemes. The structure is made of a periodic array of properly shaped glass caps infiltrated with distilled water in a two-dimensional metasurface profile, which can be easily integrated for various civilian and military applications, as well as in energy harvesting systems. Water-based metamaterials have been actively discussed for their optical transparency and good conductivity at lower frequencies, and they have been proposed both for absorbers [20] and antennas [21]. However, the absorption spectrum of water-based absorbers is typically quite limited within the existing designs [22,23]. For many civilian and defense applications, it would be highly desirable to extend the absorption band, ideally from ~1 GHz to ~100 GHz. In this work we show that, by judiciously designing a water-based moth-eye metamaterial structure, we can reach absorption levels always close to 100% in the range from 4 GHz to well above 120 GHz frequency range, in a compact profile, for incident angles from normal to grazing incidence, and for both TE and TM polarizations.

## 2. Theoretical analysis

Our concept is based on the use of distilled water contained in thin (~1 mm) glass containers shaped in a form similar to moth-eye structures. Here, of course, we use the adjective "thin" with respect to the microwave wavelength. In Fig. 1, we review the dispersion properties of water in the visible and near-IR range [24] and in the microwave range [20]. The dispersion of distilled water in the visible and near-IR can be modeled through a Sellmeier equation in Eq. (1) to fit the experimental data reported in Ref. [24], while can be modeled through the Cole-Cole equation in the microwave range [25]:

$$n = \sqrt{1 + \frac{0.75831\lambda^2}{\lambda^2 - 0.01007} + \frac{0.08495\lambda^2}{\lambda^2 - 8.91377}}. \tag{1}$$

Optics EXPRESS

$$n + iK = \sqrt{\varepsilon_\infty + \frac{\varepsilon_s - \varepsilon_\infty}{1 + \left(\frac{f}{f_r}\right)^{1-\alpha}}}. \tag{2}$$

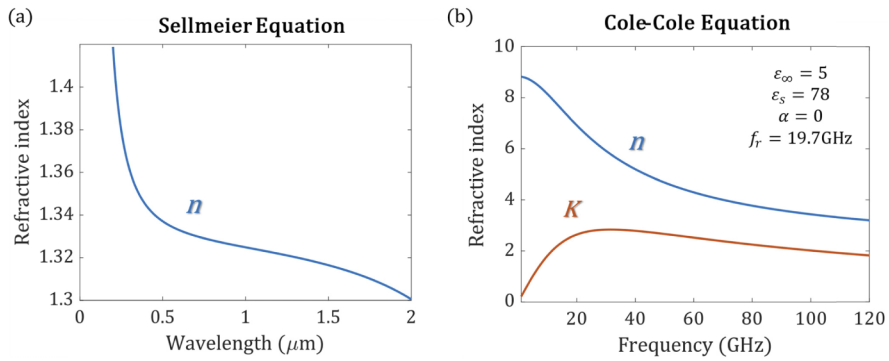


**Fig. 1.** (a) refractive index ($n$) *vs.* wavelength in the range from 0.2μm to 2μm. At these wavelengths, the extinction coefficient ($K$) is negligible. (b) $n$ and $K$ *vs.* frequency in the range from 1 GHz to 120 GHz.

As it is seen from Fig. 1, distilled water is transparent in the 0.2μm to 2μm range, but it has a large refractive index ($n$) and extinction coefficient ($K$) in the microwave range. For these reasons, it is an ideal material for our purposes.

We consider a water-based metamaterial with moth-eye geometry, as shown in Fig. 2, composed of narrow air slits carved in a water background. In order to analyze the absorption in our metamaterial, the effective permittivity $\varepsilon_{eff}$ is calculated based on the boundary conditions. For TE and TM polarized incidence, the tangential electric field and the electric current density are continuous, respectively, yielding the relation $\varepsilon_{eff} d = \varepsilon_d(d - w) + \varepsilon_0 w$, and $d/\varepsilon_{eff} = w/\varepsilon_0 + (d - w)/\varepsilon_d$ for the effective permittivity. Here, $d$ and $w$ are the period and slit width, and $\varepsilon_0$ and $\varepsilon_d$ are the permittivity of free space and water. Calculated transmission ($T$) and reflection ($R$) for a metamaterial slab of thickness $l$ are given below, where $\theta_0$, $\theta_e$ are incident and refractive angles, $l$ is the thickness of the metamaterial, $\eta_0$, $\eta_e$ and $\beta_0$, $\gamma_e$ are the impedances and propagation vectors of air and in the metamaterial:

$$R(\lambda,\, \theta_0) = \frac{\eta_e \cos\theta_0(1 + R_{23}) - \eta_0 \cos\theta_e(1 - R_{23})}{\eta_e \cos\theta_0(1 + R_{23}) + \eta_0 \cos\theta_e(1 - R_{23})}. \tag{3}$$

$$T(\lambda,\, \theta_0) = e^{j\beta_0 \cos\theta_0 l} e^{-\gamma_e \cos\theta_e l} \left[\frac{\eta_0 \cos\theta_e - \eta_e \cos\theta_0}{\eta_0 \cos\theta_e + \eta_e \cos\theta_0}\right]. \tag{4}$$

$$R_{23}(\lambda,\, \theta_0) = e^{-2\gamma_e \cos\theta_e l} \left[\frac{\eta_0 \cos\theta_e - \eta_e \cos\theta_0}{\eta_0 \cos\theta_e + \eta_e \cos\theta_0}\right]. \tag{5}$$

Here, $R_{23}$ is the reflection at the metamaterial/air interface. Figure 2(b) and 2(c) show the analytically calculated results for the absorption for TE and TM polarized input waves as a function of frequency and angle, where the absorption $A$ satisfies the usual relation: $A = 1 - |R|^2 - |T|^2$ due to power conservation. The results show that the water-based metamaterial, with period $d = 5$ mm, slit width $w = 2.5$ mm, and thickness $l = 55$ mm, absorbs the incident electromagnetic wave over a broad bandwidth and broad angular spectrum. The radiation is funneled inside the slits and totally absorbed by the water with no reflection, regardless of the high impedance mismatch that the distilled water has with respect to the incident medium (air). These analytical results suggest that the structure has the potential to achieve large absorption, close to 100%, over a broad frequency range and a broad angular spectrum for both TE and TM polarizations. In the next section, we show full-wave numerical simulations that confirm these results.

Optics EXPRESS

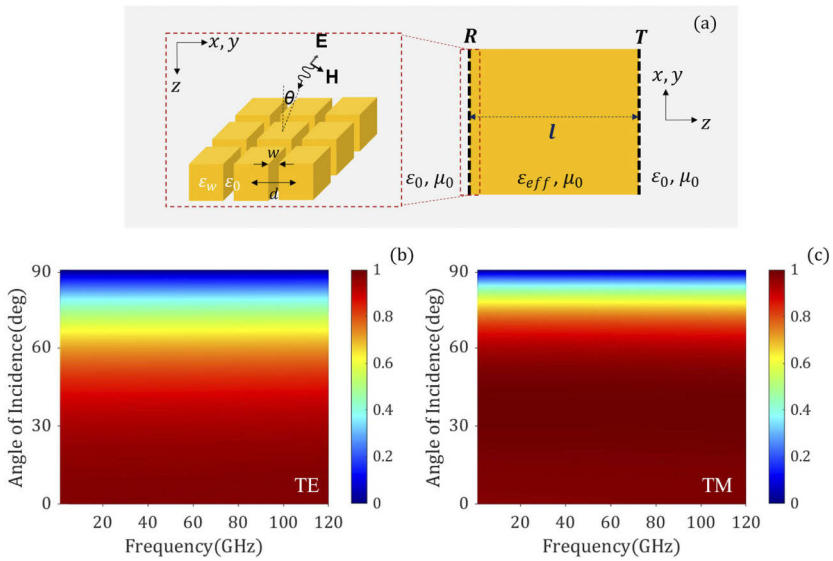


**Fig. 2.** (a) Geometry of the moth-eye metamaterial. (b-c) Analytically calculated absorption versus frequency and incidence angle for (b) TE polarization, (c) TM polarization.

## 3. Results and discussion

In Fig. 3, we show the results of a computational study carried out with a finite-difference-time-domain method [26] for a structure made of a periodic array of square cross-section pillars on a substrate, as described in Fig. 3(a). For the sake of clarity, we consider for the moment an ideally shaped structure made of water as in the theoretical analysis. We will come later to analyze a realistic structure where the water is contained in a glass cap. Analogous to the theoretical results, the metasurface shows *polarization independent, broad-angle, broadband absorption larger than 90% across most of the microwave range* with a low frequency cut-off ~7 GHz, i.e., the frequency below which the absorption starts to decrease. The low frequency cut-off can be pushed at even lower frequencies well-below 5 GHz by simply tapering the pillars, which effectively become truncated pyramids, as shown in Fig. 4. The cut-off in absorption is not reached in this plot, neither at the low frequency (5 GHz) nor at the high frequency (30 GHz) end of our simulations. This suggests that our design has the potential of absorbing over an even wider frequency range, as we show in the following. This possibility is also expected in the theoretical results of Fig. 2, where the broadband and broad-angular nature of the absorption phenomenon is achieved from 1 GHz to 120 GHz. These results confirm that our homogenization model for the moth-eye metamaterial, at the basis of the analytical results in Fig. 2, is very accurate, and captures the main physics of the problem, most importantly explaining the unusual impedance matching mechanism at the basis of the broadband absorption.

In our calculations, we have considered so far, for the sake of simplicity and clarity, a water structure without glass cover. Now, we study the realistic geometry in which distilled water is contained in a 500μm-thick borosilicate glass container. The geometrical details of the structure are shown in Fig. 5. The permittivity of the borosilicate glass in the microwave range is $\varepsilon = 4.3(1 + i0.0047)$ [25]. In Fig. 6, we simulate the absorption of the structure over a broad frequency range from 1 GHz to 120 GHz, and find that the structure indeed absorbs for most incident angles and all polarizations, with absorption levels larger than 95% up to grazing angles from ~4 GHz up to 120 GHz. The structure does not show a high frequency cut-off in absorption, suggesting that it possesses an even larger absorption bandwidth. The absorption performance

Optics EXPRESS

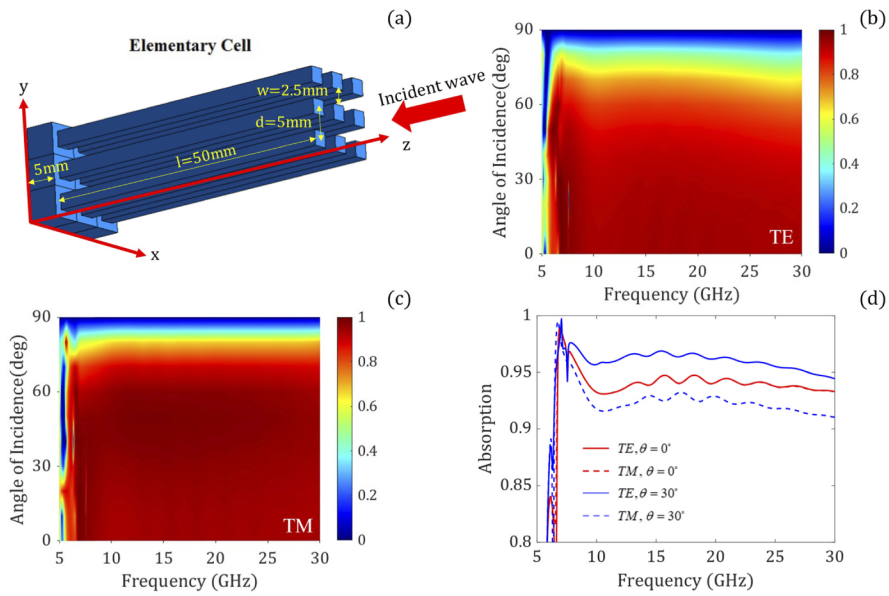


**Fig. 3.** (a) Unit cell and dimensions of the geometry of interest: $l$ is the length of the pillars, $d$ the periodicity and $w$ the slit width. (b) Absorption for TE polarization and (c) absorption for TM polarization in the (frequency, angle of incidence) plane. (d) Absorption *vs.* frequency for different incident angles and different polarizations.

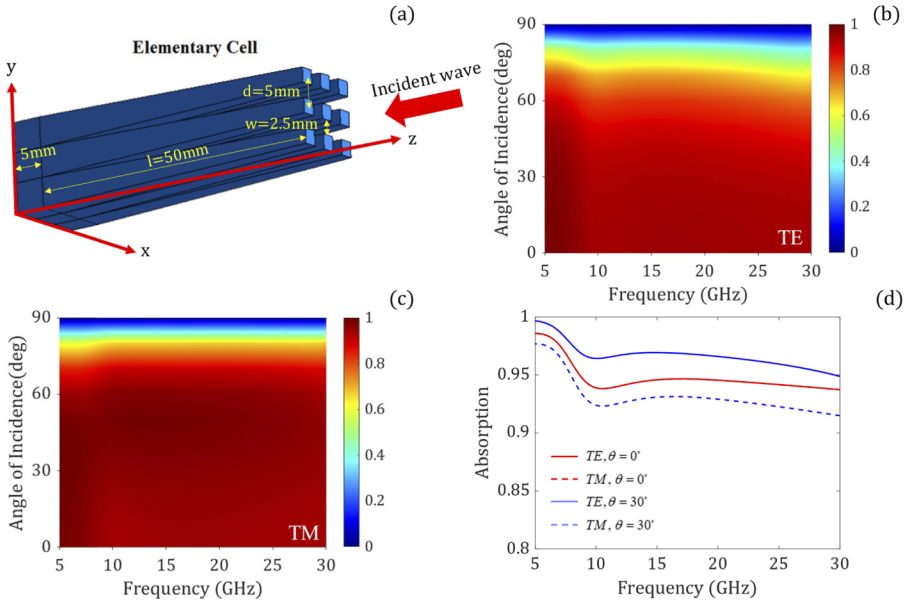


**Fig. 4.** Similar to Fig. 3, but for an array of tapered slits, formed by truncated pyramids. The tapering pushes the cut-off frequency below 5 GHz.

Optics EXPRESS

is actually improved when the glass cap is considered, compared with the uncapped case, as seen comparing Fig. 4(d) and Fig. 6(c). This is because the thin glass layer acts as a sort of antireflection coating in the microwave range, improving the overall impedance matching features of the structure.

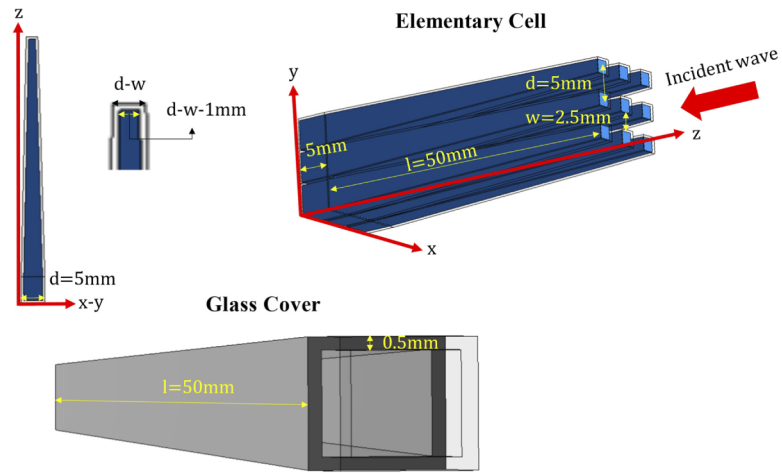


**Fig. 5.** Same as the structure described in Fig. 3(a), except that now a 500**μ**m borosilicate glass cap is included. The figure shows the geometrical details of the structure.

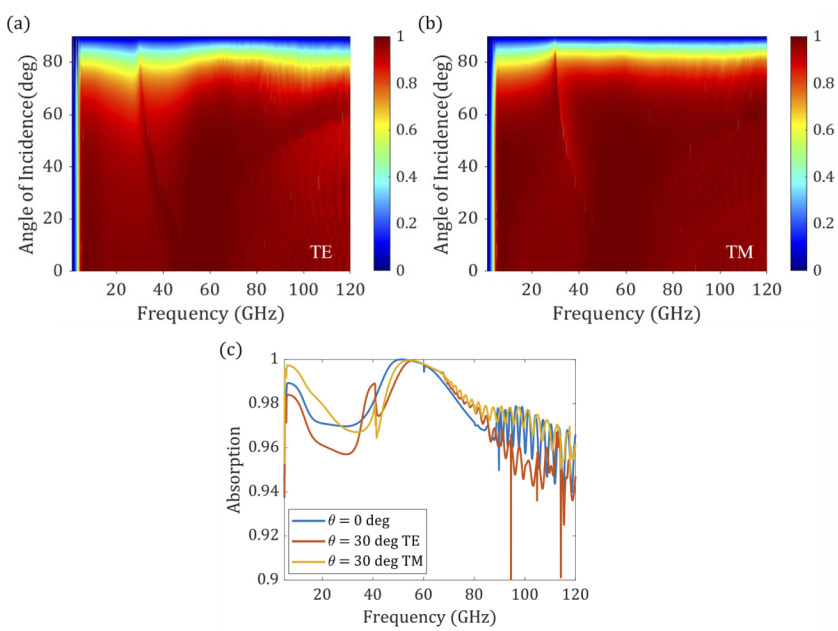


**Fig. 6.** (a) Absorption for TE polarization and (b) absorption for TM polarization in the (frequency, incident angle) plane. (c) Absorption *vs.* frequency for different incident angles and different polarizations.

To further elaborate on this unusually broad absorption mechanism, in Fig. 7 we compare the power loss density ($W/m^3$) of a simple water waveguide with glass shield and our moth-eye structure. Here, the power loss density is normalized with respect to the maximum value of power

Optics EXPRESS

loss of the moth-eye structure at the same frequency. For normal incidence, in the simple water waveguide structure most of energy is reflected and not absorbed both at 5GHz and 30GHz due to high impedance mismatch at the air/water interface. Conversely, in the moth-eye structure we can see that the electromagnetic radiation is funneled inside the slits and absorbed into the body of moth-eye structure without reflection, as a result of the effective impedance matching discussed above. The efficient absorption mechanism is facilitated by the large field concentration in the narrow air slits, as clearly evident in Fig. 7. Scanning the frequency, the region along the taper where most of the power is absorbed varies, moving downwards as the frequency is reduced. The overall thickness of the absorber fundamentally determines the lower cut-off frequency of the absorber.

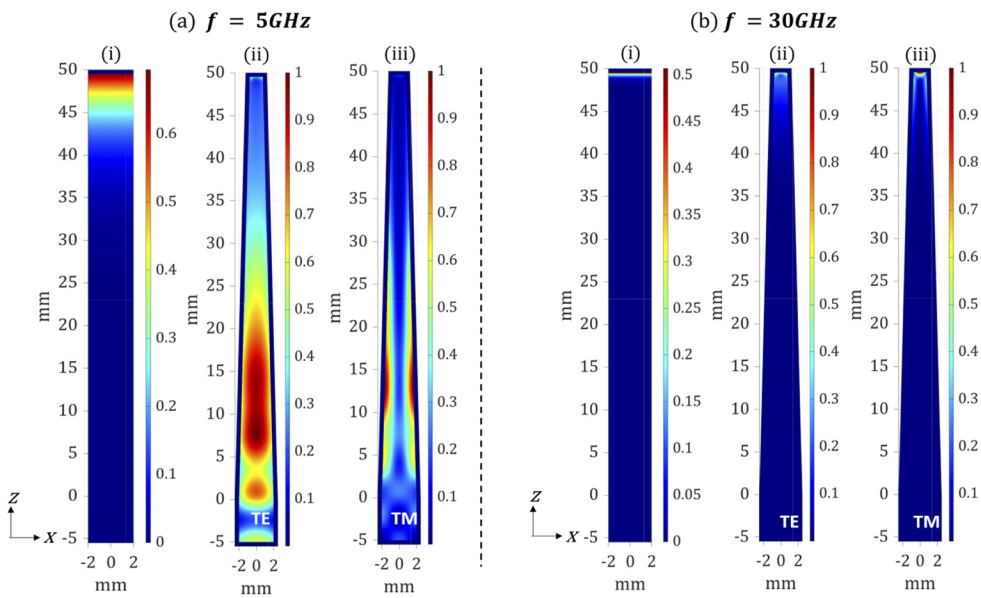


**Fig. 7.** Power loss density inside the simple water waveguide structure (a) at 5GHz radiation, (b) at 30GHz radiation (i) with glass shield and (ii), (iii) the moth-eye structure with glass cap.

Finally, we add some considerations about the transparency of the structure in the visible and near-IR range, considering the structure immersed in air. First of all, given the geometrical dimensions, we are clearly in the limit of geometrical optics at these frequencies. Second of all, both distilled water and borosilicate glass are transparent materials in the range 0.38μm to 2μm, i.e., their extinction coefficient is practically zero. Third, the refractive index difference between water ($n$~1.4) and borosilicate glass ($n$~1.5) is much smaller than the refractive index difference between air and glass at the first and last glass/air interface. Hence, we can reasonably assume that the main contribution to the reflectance of the structure comes from the Fresnel reflectance at the first and last air/glass interface. For a non-patterned structure, the transmittance is therefore given by $T \cong 1 - 2\Gamma$, where $\Gamma$ in this case is the Fresnel reflectance at the air/glass interface. For normal incidence, $\Gamma$ at an air/glass interface is approximately 4%, hence the overall transmittance would be around 92%. For a patterned structure, the reflectance at the first air/glass interface should actually be weighted by the fraction of area occupied by the glass, and therefore it should be even reduced with respect to the reflectance of the non-patterned structure. Hence, we can safely assume for our structure a transmittance level at least 90% or higher at normal incidence in the transparency range of the borosilicate glass.

Optics EXPRESS

## 4. Conclusions

In conclusion, we have proposed an effective design to realize broadband, broad-angle, polarization independent microwave absorbers that are transparent in the visible and near-IR regime. The structure is made of a periodic array of glass caps infiltrated with distilled water and shaped in the form of truncated pyramids similar to moth-eye structures. Beside glass, flexible materials, such as thermoplastic urethane, could be used as container with similar results. In discussing broadband absorbers, it is always appropriate to compare their bandwidth to the ultimate limit for passive, linear, time-invariant absorbers defined by Rozanov bound [27]. In our scenario, since the structure is open in both directions a direct comparison with this bound is not possible. However, our explorations for the same geometry discussed here with a metallic backing shows a bandwidth around 80% of the maximum limit defined in [27], which is impressive considering the relative simplicity of the design and the lack of dispersion engineering of the involved materials. Many applications, both military and civilians, such as camouflage and shielding systems or transparent energy harvesting systems, in which optically transparent absorbers are highly desirable, may benefit from our proposed design.

**Funding.** National Science Foundation; Simons Foundation; U.S. Department of Defense.

**Disclosures.** The authors declare that there are no conflicts of interest related to this article.

### References

1. P. Saville, Review of radar absorbing materials, Defence R&D Canada, Technical Memorandum, DRDC Atlantic TM 2005–003, Tech. Rep. (2005). Available at: http://www.dtic.mil/dtic/tr/fulltext/u2/a436262.pdf
2. A. N. Yusoff, M. H. Abdullah, S. H. Ahmad, S. F. Jusoh, A. A. Mansor, and S. A. Hamid, "Electromagnetic and absorption properties of some microwave absorbers," J. Appl. Phys. **92**(2), 876–882 (2002).
3. F. Qin and C. Brosseau, "A review and analysis of microwave absorption in polymer composites filled with carbonaceous particles," J. Appl. Phys. **111**(6), 061301 (2012).
4. P. Y. Chen, M. Farhat, and H. Bağcı, "Graphene metascreen for designing compact infrared absorbers with enhanced bandwidth," Nanotechnology **26**(16), 164002 (2015).
5. M. Farhat, T. Cheng, K. Q. Le, M. M. Cheng, H. Bağci, and P. Y. Chen, "Mirror-backed dark alumina: a nearly perfect absorber for thermoelectronics and thermophotovotaics," Sci. Rep. **6**(1), 19984 (2016).
6. W. W. Salisbury, US Patent No. 2599944 (1952).
7. T. Jang, H. Youn, Y. J. Shin, and L. J. Guo, "Transparent and Flexible Polarization-Independent Microwave Broadband Absorber," ACS Photonics **1**(3), 279–284 (2014).
8. W. Zhang, P. H. Q. Pham, E. R. Brown, and P. J. Burke, "AC conductivity parameters of graphene derived from THz etalon transmittance," Nanoscale **6**(22), 13895–13899 (2014).
9. B. Wu, H. M. Tuncer, M. Naeem, B. Yang, M. T. Cole, W. I. Milne, and Y. Hao, "Experimental demonstration of a transparent graphene millimeter wave absorber with 28% fractional bandwidth at 140 GHz," Sci. Rep. **4**(1), 4130 (2015).
10. Y. Okano, S. Ogino, and K. Ishikawa, "Development of Optically Transparent Ultrathin Microwave Absorber for Suppression of Misidentification Possibility of UHF-RFID System," Electron. Commun. Jpn. **98**(1), 36–46 (2015).
11. O. Balci, E. O. Polat, N. Kakenov, and C. Kocabas, "Graphene-enabled electrically switchable radar-absorbing surfaces," Nat. Commun. **6**(1), 6628 (2015).
12. M. Grande, G. V. Bianco, M. A. Vincenti, D. de Ceglia, P. Capezzuto, M. Scalora, G. Bruno, and A. D'Orazio, "Optically transparent microwave screens based on engineered graphene layers," Opt. Express **24**(20), 22788–22795 (2016).
13. L. Rayleigh, "On reflection of vibrations at the confines of two media between which the transition is gradual," Proc. London Math. Soc. **s1-11**(1), 51–56 (1879).
14. C. G. Bernhard and W. H. Miller, "A corneal nipple pattern in insect compound eyes," Acta Physiol. Scand. **56**(3-4), 385–386 (1962).
15. D. G. Stavenga, S. Foletti, G. Palasantzas, and K. Arikawa, "Light on the moth-eye corneal nipple array of butterflies," Proc. R. Soc. London, Ser. B **273**(1587), 661–667 (2006).
16. S. A. Boden and D. M. Bagnall, "Optimization of moth-eye antireflection schemes for silicon solar cells," Prog. Photovoltaics **18**(3), 195–203 (2010).
17. Y. Ou, D. Corell, C. Dam-Hansen, P. Petersen, and H. Ou, "Antireflective sub-wavelength structures for improvement of the extraction efficiency and color rendering index of monolithic white light-emitting diode," Opt. Express **19**(S2), A166–A172 (2011).
18. R. J. Weiblen, C. R. Menyuk, L. E. Busse, L. B. Shaw, J. S. Sanghera, and I. D. Aggarwal, "Optimized moth-eye anti-reflective structures for $As_2S_3$ chalcogenide optical fibers," Opt. Express **24**(10), 10172–10187 (2016).

Optics EXPRESS


19. R. Contractor, G. D'Aguanno, and C. R. Menyuk, "Ultra-broadband, polarization-independent, wide-angle absorption in impedance-matched metamaterials with anti-reflective moth-eye surfaces," Opt. Express **26**(18), 24031–24043 (2018).
20. Z. Wu, X. Chen, Z. Zhang, L. Heng, S. Wang, and Y. Zou, "Design and optimization of a flexible water-based microwave absorbing metamaterial," Appl. Phys. Express **12**(5), 057003 (2019).
21. J. Sun and K. Luk, "A Wideband and Optically Transparent Water Patch Antenna with Broadside Radiation Pattern," IEEE Antennas Wirel. Propag. Lett. **19**(2), 341–345 (2020).
22. H. Xiong and F. Yang, "Ultra-broadband and tunable saline water-based absorber in microwave regime," Opt. Express **28**(4), 5306–5316 (2020).
23. J. Zhao, S. Wei, C. Wang, K. Chen, B. Zhu, T. Jiang, and Y. Feng, "Broadband microwave absorption utilizing water-based metamaterial structures," Opt. Express **26**(7), 8522–8531 (2018).
24. G. M. Hale and M. R. Querry, "Optical Constants of Water in the 200-nm to 200-(m Wavelength Region," Appl. Opt. **12**(3), 555–563 (1973).
25. K. Fenske and D. Misra, "Dielectric Materials at Microwave Frequencies," Appl. Microwave and Wireless **12**(10), 92–100 (2000).
26. CST Studio Suite 2018, https://www.3ds.com/.
27. K. N. Rozanov, "Ultimate thickness to bandwidth ratio of radar absorbers," IEEE Trans. on Antenna and Propagation **48**(8), 1230–1234 (2000).